A CONVEX VARIATIONAL MODEL FOR RESTORING BLURRED IMAGES WITH MULTIPLICATIVE NOISE

YIQIU DONG* AND TIEYONG ZENG †

Abstract. In this paper, a new variational model for restoring blurred images with multiplicative noise is proposed. Based on the statistical property of the noise, a quadratic penalty function technique is utilized in order to obtain a strictly convex model under a mild condition, which guarantees the uniqueness of the solution and the stabilization of the algorithm. For solving the new convex variational model, a primal-dual method is proposed and its convergence is studied. The paper ends with a report on numerical tests for the simultaneous deblurring and denoising of images subject to multiplicative noise. A comparison with other methods is provided as well.

Key words. Convexity, deblurring, multiplicative noise, primal-dual method, total variation regularization, variational model.

AMS subject classifications. 52A41, 65K10, 65K15, 90C30, 90C47

1. Introduction. In real applications, degradation effects are unavoidable during image acquisition and transmission. For instance, the photos produced by astronomical telescopes are often blurred by atmospheric turbulence. In order to benefit further image processing tasks, image deblurring and denoising continue to attract the attentions in the applied mathematics community. Based on the imaging systems, various kinds of noise were considered, such as additive Gaussian noise, impulse noise, and Poisson noise, etc. We refer the reader to [14,17,28,33,37,38] and references therein for an overview of those noise models and the restoration methods. However, multiplicative noise is a different noise model, and it commonly appears in synthetic aperture radar (SAR), ultrasound imaging, laser images, and so on [5, 6, 32, 36]. For a mathematical description of such degradations, suppose that an image $\hat{u}$ is a real function defined on Ω, a connected bounded open subset of $\mathbb{R}^2$ with compact Lipschitz boundary, i.e., $\hat{u} : \Omega \to \mathbb{R}$. The degraded image f is given by:

$$f = (A\hat{u})\eta, \tag{1.1}$$

where $A \in \mathcal{L}(L^2(\Omega))$ is a known linear and continuous blurring operator, and η represents multiplicative noise with mean 1. Here, f is blurred by the blurring operator A, and then is corrupted by the multiplicative noise η. Usually we assume that $f > 0$. In this paper, we concentrate on the assumption that η follows a Gamma distribution, which commonly occurs in SAR. The deblurring process under noise is well-known to be an ill-posed problem in the sense of Hadamard [25]. Since the degraded image only provides partial restrictions on the original data, there exist various solutions which can match the observed degraded image under the given blurring operator. Hence, in order to utilize variational method, the main challenge in image restoration is to design a reasonable and easily solved optimization problem based on the degradation model and the prior information on the original image.

Until the past decade, a few variational methods have been proposed to handle the restoration problem with the multiplicative noise. Given the statistical properties

*Institute of Biomathematics and Biometry, Helmholtz Zentrum München, Ingolstädter Landstrasse 1, 85764 Neuherberg, Germany. (yiqiu.dong@helmholtz-muenchen.de)

†Department of Mathematics, Hong Kong Baptist University, Kowloon Tong, Hong Kong. (zeng@hkbu.edu.hk)

of the multiplicative noise η, in [32] the recovery of the image $\hat{u}$ was based on solving the following constrained optimization problem:

$$\begin{array}{ll} \inf\limits_{u \in S(\Omega)} & \int_\Omega |Du| \\ \text{subject to:} & \int_\Omega \frac{f}{Au}\, dx = 1 \\ & \int_\Omega (\frac{f}{Au} - 1)^2\, dx = \theta^2, \end{array} \tag{1.2}$$

where θ^2 denotes the variance of η, $S(\Omega) = \{v \in BV(\Omega) : v > 0\}$, $BV(\Omega)$ is the space of functions of bounded variation (see [4] or below), and the total variation (TV) of u is utilized as the objective function in order to preserve significant edges in images. In (1.2), only basic statistical properties, the mean and the variance, of the noise η are considered, which somehow limits the restored results. For this reason, based on the Bayes rule and Gamma distribution with mean 1, by using a maximum a posteriori (MAP) estimator Aubert and Aujol [3] introduced a variational model as follows:

$$\inf_{u \in S(\Omega)} \int_\Omega \left(\log(Au) + \frac{f}{Au} \right)\, dx + \lambda \int_\Omega |Du|, \tag{1.3}$$

where the TV of u is utilized as the regularization term, and $\lambda > 0$ is the regularization parameter which controls the trade-off between a good fit of f and a smoothness requirement due to the TV regularization. Since both (1.2) and (1.3) are non-convex, the gradient projection algorithms proposed in [32] and [3] may stick at some local minimizers, and the restoration results strongly rely on the initialization and the numerical schemes.

To overcome this problem and provide a convex model, in [26] Huang et al. introduced an auxiliary variable $z = \log u$ in (1.3), and in [34] Shi et al. modified (1.3) by adding a quadratic term. With convex models, these two methods both provide better restored results than the method proposed in [3], and they are independent of the initial estimation. In addition, Steidl et al. combined the I-divergence as the data fidelity term with the TV regularization or the nonlocal means to remove the multiplicative Gamma noise [35]. In [18], the denoising problem was handled by using L^1 fidelity term on frame coefficients. In [29], the approach with spatially varying regularization parameters in the AA model was considered in order to restore more texture details of the denoised image. However, all of the above methods only work on the multiplicative noise removal issue, and it is still an open question to extend them to the deblurring case.

In this paper, we focus on the restoration of images that are simultaneously blurred and also corrupted by multiplicative noise. Since the non-convexity of the model (1.3) proposed in [3] causes uniqueness problem and the issue of convergence of the numerical algorithm, we introduce a new convex model by adding a quadratic penalty term based on the statistical properties of the multiplicative Gamma noise. Furthermore, we study the existence and uniqueness of a solution to the new model on the continuous, i.e. functional space, level. Here, we still use the TV regularization in order to preserving edges during the reconstruction. Evidently, it can be readily extended to some other modern regularization terms such as non-local TV [21] or framelet approach [9]. The minimization problem in our method is solved by the primal-dual algorithm proposed in [12, 19] instead of the gradient projection method in [3, 32]. The numerical results in this paper show that our method has the potential to outperform the other approaches in multiplicative noise removal with deblurring simultaneously.

The rest of the paper is organized as follows. In Section 2, we briefly review the total variation regularization and provides its main properties. In Section 3, based on the statistical properties of the multiplicative Gamma noise we propose a new convex model for denoising, and study its existence and uniqueness of a solution with several other properties. Then in Section 4 we extend the model and those properties to the case of denoising and deblurring simultaneously. Section 5 gives the primal-dual algorithm for solving our restoration model based on the work proposed in [12]. The numerical results shown in Section 6 demonstrate the affectivity of the new method. Finally, conclusions are drawn in Section 7.

2. Review of Total Variation Regularization. In order to preserve significant edges in images, in their seminal work [33] Rudin et al. introduced total variation regularization into image restoration. In this approach, they recover the image in $BV(\Omega)$, which denotes the space of functions of bounded variation, i.e. $u \in BV(\Omega)$ iff $u \in L^1(\Omega)$ and the BV-seminorm:

$$\int_\Omega |Du| := \sup\left\{\int_\Omega u\cdot \operatorname{div}(\xi(x))dx \big| \xi \in C_0^\infty(\Omega,\mathbb{R}^2), \|\xi\|_{L^\infty(\Omega,\mathbb{R}^2)} \leq 1\right\}, \tag{2.1}$$

is finite. The space $BV(\Omega)$ endowed with the norm $\|u\|_{BV} = \|u\|_{L^1} + \int_\Omega |Du|$ is a Banach space. If $u \in BV(\Omega)$, the distributional derivative Du is a bounded Radon measure and the above quantity defined in (2.1) corresponds to the total variation (TV). Based on the compactness of $BV(\Omega)$, in two-dimensional case we have the embedding $BV(\Omega) \hookrightarrow L^p(\Omega)$ for $1 \leq p \leq 2$ which are compact for $p < 2$. See [1, 4, 13] for more details.

3. A Convex Multiplicative Denoising Model. To propose a convex multiplicative denoising model, we start from the multiplicative Gamma noise. Suppose that the random variable η follows Gamma distribution, i.e., its probability density function is:

$$p_\eta(x;\theta,K) = \frac{1}{\theta^K\Gamma(K)}x^{K-1}e^{-\frac{x}{\theta}} \quad \text{for} \quad x \geq 0, \tag{3.1}$$

where Γ is the usual Gamma-function, θ and K denote the scale and shape parameters in the Gamma distribution, respectively. Furthermore, the mean of η is $K\theta$, and the variance of η is $K\theta^2$, see [24]. As multiplicative noise, in general we assume that the mean of η equals 1, then we have that $K\theta = 1$ and its variance is $\frac{1}{K}$. Now, set a random variable $Y = \frac{1}{\sqrt{\eta}}$. Inspired by the central limit theorem [30], it is interesting to approximate Y by the Gaussian distribution, and we have the following results.

PROPOSITION 3.1. *Suppose that the random variable η is of Gamma distribution with mean 1. Set $Y = \frac{1}{\sqrt{\eta}}$. Then the means of Y and Y^2 are:*

$$\mathbb{E}(Y) = \frac{\sqrt{K}\Gamma(K-1/2)}{\Gamma(K)} \quad \text{and} \quad \mathbb{E}(Y^2) = \frac{K}{K-1},$$

respectively.

Proof. Based on the probability density function of η shown in (3.1) and $K\theta = 1$, we obtain:

$$
\begin{aligned}
\mathbb{E}(Y) &= \int_0^{+\infty} \frac{1}{\sqrt{x}} \frac{1}{\theta^K \Gamma(K)} x^{K-1} e^{-\frac{x}{\theta}}\ dx \\
&= \frac{\Gamma(K-1/2)}{\sqrt{\theta}\Gamma(K)} \int_0^{+\infty} \frac{1}{\theta^{K-1/2}\Gamma(K-1/2)} x^{K-3/2} e^{-\frac{x}{\theta}}\ dx \\
&= \frac{\Gamma(K-1/2)}{\sqrt{\theta}\Gamma(K)} \int_0^{+\infty} p_\eta(x;\theta, K-1/2)\ dx \\
&= \frac{\sqrt{K}\Gamma(K-1/2)}{\Gamma(K)}.
\end{aligned}
$$

Similarly, we have:

$$
\begin{aligned}
\mathbb{E}(Y^2) &= \int_0^{+\infty} \frac{1}{x} \frac{1}{\theta^K \Gamma(K)} x^{K-1} e^{-\frac{x}{\theta}} dx \\
&= \frac{\Gamma(K-1)}{\theta\Gamma(K)} \int_0^{+\infty} \frac{1}{\theta^{K-1}\Gamma(K-1)} x^{K-2} e^{-\frac{x}{\theta}} dx \\
&= \frac{K}{K-1}.
\end{aligned}
$$

□

According to the properties of Gamma function [2] and Proposition 3.1, if K is large, the mean of Y, $\mathbb{E}(Y)$, approximates to $\sqrt{\frac{K}{K-\frac{1}{2}}}$, and is close to 1. Since generally the value of K is unknown, we use 1 as the approximation of $\mathbb{E}(Y)$. In our numerical practice this setting turns out to yield reliable results. Furthermore, considering the denoising case, that is, A is the identity operator, from the degradation model (1.1), we obtain that $Y = \frac{1}{\sqrt{\eta}} = \sqrt{\frac{u}{f}}$, which follows the Gaussian distribution approximately. In order to reduce the influence on the restored results from noise, we propose the following multiplicative denoising model:

$$
\inf_{u \in \bar{S}(\Omega)} E(u) := \int_\Omega \left(\log u + \frac{f}{u} \right)\ dx + \alpha \int_\Omega \left(\sqrt{\frac{u}{f}} - 1 \right)^2\ dx + \lambda \int_\Omega |Du|, \tag{3.2}
$$

where the second term is associated with the variance of $\sqrt{\frac{u}{f}}$, and its parameter $\alpha > 0$. In addition, we set:

$$
\bar{S}(\Omega) := \{v \in BV(\Omega) : v \geq 0\},
$$

which is closed and convex, and we define $\log 0 = -\infty$ and $\frac{1}{0} = +\infty$. Note that as $f > 0$, we need not define $\frac{0}{0}$.

3.1. Existence and uniqueness of a solution. For the existence and uniqueness of a solution to (3.2), we start by discussing the convexity of the model. Since the quadratic penalty term provides extra convexity, we can prove that $E(u)$ in (3.2) is convex, if the parameter α satisfies certain condition.

PROPOSITION 3.2. *If* $\alpha \geq \frac{2\sqrt{6}}{9}$, *then the model* (3.2) *is strictly convex.*

Proof. With $t \in \mathbb{R}^+$ and a fixed α, we define a function g as:

$$
g(t) := \log t + \frac{1}{t} + \alpha(\sqrt{t} - 1)^2.
$$

Easily, we have that the second order derivative of g satisfies:

$$g''(t) = -t^{-2} + 2t^{-3} + \frac{\alpha}{2} t^{-\frac{3}{2}}.$$

A direct computation shows that the function g'' reaches to its unique minimum, $\frac{3\sqrt{6}\alpha - 4}{6^3}$, at $t = 6$. Hence, if $\alpha \geq \frac{2\sqrt{6}}{9}$, we have $g''(t) \geq 0$, i.e., g is convex. Furthermore, since the function g has only one minimizer, g is strictly convex when $\alpha \geq \frac{2\sqrt{6}}{9}$.

Setting $t = \frac{u(x)}{f(x)}$ for each $x \in \Omega$, we obtain the strict convexity of the first two terms in (3.2). Based on the convexity of the TV regularization, we deduce that $E(u)$ in (3.2) is strictly convex, if $\alpha \geq \frac{2\sqrt{6}}{9}$. Since the feasible set $\bar{S}(\Omega)$ is convex, the assertion is an immediate consequence. ◻

Based on Proposition 3.2, we see that with a suitable α, (3.2) is a convex approximation of the non-convex model (1.3) with A as the identity operator. Now, we argue the existence and uniqueness of a solution to (3.2) and the maximum principle.

THEOREM 3.3. *Let f be in $L^\infty(\Omega)$ with $\inf_\Omega f > 0$, then the model* (3.2) *has a solution u^* in $BV(\Omega)$ satisfying:*

$$0 < \inf_\Omega f \leq u^* \leq \sup_\Omega f.$$

Moreover, if $\alpha \geq \frac{2\sqrt{6}}{9}$, the solution of (3.2) *is unique.*

Proof. Set $c_1 := \inf_\Omega f$, $c_2 := \sup_\Omega f$, and let:

$$E_0(u) := \int_\Omega \left(\log u + \frac{f}{u} \right) \, dx + \alpha \int_\Omega \left(\sqrt{\frac{u}{f}} - 1 \right)^2 \, dx.$$

Noting that $E(u)$ in (3.2) is bounded from below, we can choose a minimizing sequence $\{u_n : n = 1, 2, \cdots\} \in \bar{S}(\Omega)$.

Since for each fixed $x \in \Omega$, the real function on $\mathbb{R}^+$:

$$g(t) := \log t + \frac{f(x)}{t} + \alpha \left(\sqrt{\frac{t}{f(x)}} - 1 \right)^2,$$

is decreasing if $t \in (0, f(x))$ and increasing if $t \in (f(x), +\infty)$, one always has $g(\min(t, M)) \leq g(t)$ with $M \geq f(x)$. Hence, we obtain that:

$$E_0(\inf(u, c_2)) \leq E_0(u).$$

Combining with $\int_\Omega |D \inf(u, c_2)| \leq \int_\Omega |Du|$, see Lemma 1 in section 4.3 of [27], we have $E(\inf(u, c_2)) \leq E(u)$. In the same way we are able to get $E(\sup(u, c_1)) \leq E(u)$. Hence, we can assume that $0 < c_1 \leq u_n \leq c_2$, which implies that u_n is bounded in $L^1(\Omega)$.

As $\{u_n\}$ is a minimizing sequence, we know that $E(u_n)$ is bounded. Furthermore, $\int_\Omega |Du_n|$ is bounded, and $\{u_n\}$ is bounded in $BV(\Omega)$. Therefore, there exists a subsequence $\{u_{n_k}\}$ which converges strongly in $L^1(\Omega)$ to some $u^* \in BV(\Omega)$, and $\{Du_{n_k}\}$ converges weakly as a measure to Du^* [4]. Since $\bar{S}(\Omega)$ is closed and convex, by the lower semi-continuity of the total variation and Fatou's lemma, we get that u^* is a solution of the model (3.2), and necessarily $0 < c_1 \leq u^* \leq c_2$.

Moreover,if $\alpha \geq \frac{2\sqrt{6}}{9}$, uniqueness follows directly from the strict convexity of the function E. ◻

In [3] a comparison principle was given concerning the model (1.3). With the α-term in (3.2), the comparison principle is satisfied with certain condition on α.

PROPOSITION 3.4. *Let f_1 and f_2 be in $L^\infty(\Omega)$ with $a_1 > 0$ and $a_2 > 0$, where $a_1 = \inf_\Omega f_1$ and $a_2 = \inf_\Omega f_2$. Further, set $b_1 = \sup_\Omega f_1$ and $b_2 = \sup_\Omega f_2$. Assume $f_1 < f_2$. Suppose u_1^* (resp. u_2^*) is a solution of (3.2) with $f = f_1$ (resp. $f = f_2$). Then when $\alpha < \frac{a_1 a_2}{b_1 b_2 - a_1 a_2}$, we have $u_1 \leq u_2$.*

Proof. Referring to [3], we define $u \wedge v = \inf(u, v)$ and $u \vee v = \sup(u, v)$. Since u_i^* is a minimizer of $E(u)$ defined in (3.2) with f_i with respect to $i = 1, 2$, we have:

$$E(u_1^* \wedge u_2^*) + E(u_1^* \vee u_2^*) \geq E(u_1^*) + E(u_2^*).$$

Based on the result $\int_\Omega |D(u_1^* \wedge u_2^*)| + \int_\Omega |D(u_1^* \vee u_2^*)| \leq \int_\Omega |Du_1^*| + \int_\Omega |Du_2^*|$ in [10,22], we get:

$$\begin{aligned}
&\int_\Omega \left[\log(u_1^* \wedge u_2^*) + \frac{f_1}{u_1^* \wedge u_2^*} + \alpha \left(\sqrt{\frac{u_1^* \wedge u_2^*}{f_1}} - 1 \right)^2 \right] dx \\
&\qquad + \int_\Omega \left[\log(u_1^* \vee u_2^*) + \frac{f_2}{u_1^* \vee u_2^*} + \alpha \left(\sqrt{\frac{u_1^* \vee u_2^*}{f_2}} - 1 \right)^2 \right] dx \\
&\qquad\qquad \geq \int_\Omega \left[\log u_1^* + \frac{f_1}{u_1^*} + \alpha \left(\sqrt{\frac{u_1^*}{f_1}} - 1 \right)^2 \right] dx \\
&\qquad\qquad\qquad + \int_\Omega \left[\log u_2^* + \frac{f_2}{u_2^*} + \alpha \left(\sqrt{\frac{u_2^*}{f_2}} - 1 \right)^2 \right] dx.
\end{aligned}$$

Writing $\Omega = \{u_1^* > u_2^*\} \cup \{u_1^* \leq u_2^*\}$, we easily deduce that:

$$\int_{\{u_1^* > u_2^*\}} (f_1 - f_2)(u_1^* - u_2^*) \left[\frac{1}{u_1^* u_2^*} + \frac{\alpha}{f_1 f_2} - \frac{2\alpha}{\sqrt{f_1 f_2}(\sqrt{f_1} + \sqrt{f_2})(\sqrt{u_1^*} + \sqrt{u_2^*})} \right] \geq 0.$$

Based on Theorem 3.3, we have $0 < a_1 \leq u_1^* \leq b_1$ and $0 < a_2 \leq u_2^* \leq b_2$, which imply $\frac{1}{u_1^* u_2^*} \geq \frac{1}{b_1 b_2}$ and:

$$\frac{2}{\sqrt{f_1 f_2}(\sqrt{f_1} + \sqrt{f_2})(\sqrt{u_1^*} + \sqrt{u_2^*})} - \frac{1}{f_1 f_2} \leq \frac{2}{\sqrt{a_1 a_2}(\sqrt{a_1} + \sqrt{a_2})^2} - \frac{1}{b_1 b_2} \leq \frac{1}{a_1 a_2} - \frac{1}{b_1 b_2}.$$

Hence, we find that:

$$\frac{1}{u_1^* u_2^*} + \frac{\alpha}{f_1 f_2} - \frac{2\alpha}{\sqrt{f_1 f_2}(\sqrt{f_1} + \sqrt{f_2})(\sqrt{u_1^*} + \sqrt{u_2^*})} > 0,$$

as soon as $\alpha < \frac{a_1 a_2}{b_1 b_2 - a_1 a_2}$. Taking account of $f_1 < f_2$, in this case we deduce that $\{u_1^* > u_2^*\}$ has a zero Lebesgue measure, i.e. $u_1^* \leq u_2^*$ a.e. in Ω. □

4. The Extension to Simultaneous Deblurring and Denoising. The model (3.2) is based on the statistical properties of Gamma distribution, and is specifically devoted to the multiplicative Gamma noise removal. In this section, we extend it to the simultaneous deblurring and denoising case, i.e., to restore the image $\hat{u}$ in (1.1) with the blurring operator A. The restoration is processed by solving the optimization problem:

$$\inf_{u\in\bar{S}(\Omega)} E_A(u) := \int_\Omega \left(\log Au + \frac{f}{Au}\right)\, dx + \alpha \int_\Omega \left(\sqrt{\frac{Au}{f}} - 1\right)^2 \, dx + \lambda \int_\Omega |Du|, \quad (4.1)$$

where $A \in \mathcal{L}(L^2(\Omega))$. As a blurring operator, we assume that A is a nonnegative operator, i.e., $A \geq 0$ in short. Then we have $Au \geq 0$ with $u \in \bar{S}(\Omega)$. Similar as Proposition 3.2, since A is linear, we can readily establish the following convexity result.

PROPOSITION 4.1. *If $\alpha \geq \frac{2\sqrt{6}}{9}$, then the model (4.1) is convex.*

4.1. Existence of a solution. Based on the properties of total variation and the space of bounded variation functions, we prove the existence and uniqueness of a solution to (4.1).

THEOREM 4.2. *Recall that $\Omega \subset \mathbb{R}^2$ is a connected bounded set with compact Lipschitz boundary. Suppose that $A \in \mathcal{L}(L^2(\Omega))$ is nonnegative, and it does not annihilate constant functions, i.e., $A1 \neq 0$. Let f be in $L^\infty(\Omega)$ with $\inf_\Omega f > 0$, then the model (4.1) admits a solution u^*. Moreover, if $\alpha \geq \frac{2\sqrt{6}}{9}$ and A is injective, then the solution is unique.*

Proof. We note that E_A is bounded from below, then choose a minimizing sequence $\{u_n\} \in \bar{S}(\Omega)$ for (4.1). So $\{\int_\Omega |Du_n|\}$ with $n = 1, 2, \cdots$ is bounded. Using the Poincaré inequality (see Remark 3.50, [1]), we obtain:

$$\|u_n - m_\Omega(u_n)\|_2 \leq C \int_\Omega |D(u_n - m_\Omega(u_n))| = C \int_\Omega |Du_n|, \quad (4.2)$$

where $m_\Omega(u_n) = \frac{1}{|\Omega|}\int_\Omega u_n \, dx$ with $|\Omega|$ denotes the measure of Ω, and C is a constant. Recalling that Ω is bounded, it follows that $\|u_n - m_\Omega(u_n)\|_2$ is bounded for each n. Since $A \in \mathcal{L}(L^2(\Omega))$ is continuous, $\{A(u_n - m_\Omega(u_n))\}$ must be bounded in $L^2(\Omega)$ and in $L^1(\Omega)$.

On the other hand, according to the boundedness of $E_A(u_n)$, for each n $\left(\sqrt{\frac{Au_n}{f}} - 1\right)^2$ is bounded in $L^1(\Omega)$, which implies that $\left\|\frac{Au_n}{f}\right\|_1$ is bounded, then we obtain that $\|Au_n\|_1$ is bounded. Moreover, we have:

$$|m_\Omega(u_n)| \cdot \|A1\|_1 = \|A(u_n - m_\Omega(u_n)) - Au_n\|_1 \leq \|A(u_n - m_\Omega(u_n))\|_1 + \|Au_n\|_1.$$

Hence, $|m_\Omega(u_n)| \cdot \|A1\|_1$ is bounded. Thanks to $A1 \neq 0$, we obtain that $m_\Omega(u_n)$ is uniformly bounded. Together with the boundedness of $\{u_n - m_\Omega(u_n)\}$, it leads to the boundedness of $\{u_n\}$ in $L^2(\Omega)$ and thus in $L^1(\Omega)$. Since $\bar{S}(\Omega)$ is closed and convex, $\{u_n\}$ is bounded in $\bar{S}(\Omega)$ as well.

Therefore, there exists a subsequence $\{u_{n_k}\}$ which converges weakly in $L^2(\Omega)$ to some $u^* \in L^2(\Omega)$, and $\{Du_{n_k}\}$ converges weakly as a measure to Du^*. Due to the continuity of the linear operator A, one must have that $\{Au_{n_k}\}$ converges weakly to Au^* in $L^2(\Omega)$. Then based on the lower semi-continuity of the total variation and Fatou's lemma, we obtain that u^* is a solution of the model (4.1).

Based on Proposition 4.1, when $\alpha \geq \frac{2\sqrt{6}}{9}$, the model (4.1) is convex. Furthermore, if A is injective, (4.1) is strictly convex, then its minimizer has to be unique. □

REMARK 4.3. *In the proof of Theorem 4.2, because of the α-term, we obtain that the sequence $\{Au_n\}$ is bounded in $L^1(\Omega)$. Thus, when $\alpha = 0$, that is, in the case of the* *model* (1.3)*, it is difficult to get the same result, and in [3] the existence of a solution to* (1.3) *is still an open question.*

According to the constraint in (4.1), we find that its minimizer is nonnegative. Further, we have the following result.

PROPOSITION 4.4. *Suppose that* u^* *is the solution of* (4.1)*. For any* $0 < \epsilon < 1$*, there exists a constant* C_1 *such that:*

$$|\{x \in \Omega : (Au^*)(x) \leq \epsilon f(x)\}| \leq \frac{\epsilon}{1 + \epsilon \log \epsilon} \left(C_1 + \int_\Omega \log f \ dx \right).$$

Proof. Suppose that C_1 is the minimal value of (4.1). Set $w = \frac{Au^*}{f}$, then we have:

$$|\Omega| + \int_\Omega \log f \ dx \leq \int_\Omega \left(\log w + \frac{1}{w} \right) \ dx \leq C_1 + \int_\Omega \log f \ dx,$$

where we have used the fact that for each $t > 0$, $\log t + \frac{1}{t} \geq 1$. Moreover, if $t \leq \epsilon < 1$, then $\log t + \frac{1}{t} \geq \log \epsilon + \frac{1}{\epsilon}$, we then get that:

$$|\{x \in \Omega : w(x) \leq \epsilon\}| \leq \frac{\epsilon}{1 + \epsilon \log \epsilon} \left(C_1 + \int_\Omega \log f \ dx \right).$$

Then based on $w = \frac{Au^*}{f}$, we obtain the assertion. □

As a consequence, $|\{x \in \Omega : (Au^*)(x) = 0\}| = 0$, i.e., Au^* is positive almost everywhere. Especially, in the discrete situation, Au^* is strictly positive.

4.2. Bias correction. Let us write down the classical ROF model proposed in [33]:

$$\inf_{u \in BV(\Omega)} \int_\Omega \frac{1}{2}(Au - f)^2 \ dx + \lambda \int_\Omega |Du|, \tag{4.3}$$

where $\lambda > 0$ is the regularization parameter, and f is degraded image with Gaussian noise. Readily, under mild condition, the solution of (4.3) exists. Denote u^* as a solution of (4.3) and recall that $m_\Omega(u)$ denotes the mean value of u over Ω. Through the theoretical analysis in [11, 13], we have that the mean value of the solution preserves automatically, i.e., $m_\Omega(Au^*) = m_\Omega(f)$.

In [18], a bias correction step for multiplicative noise removal is proposed. Evidently, for our new model (4.1) which addresses delurring with denoising simultaneously, we need some substantial investigation.

PROPOSITION 4.5. *Suppose that* $A1 = 1$*. Let* u^* *be a solution of* (4.1)*, then the following properties hold true:*

(i)

$$\int_\Omega \left[\frac{f}{(Au^*)^2} - \alpha \left(\frac{1}{f} - \frac{1}{\sqrt{f \cdot Au^*}} \right) \right] \ dx = \int_\Omega \frac{1}{Au^*} \ dx.$$

(ii) If there exists a solution in the case of $\alpha = 0$*, then we have,*

$$\int_\Omega \frac{1}{f} \ dx \geq \int_\Omega \frac{1}{Au^*} \ dx.$$

Proof.

(i) We define a function with single nonnegative variable $t \in \mathbb{R}$:

$$e(t) := \int_\Omega \left(\log A(u^* + t) + \frac{f}{A(u^* + t)} \right) \, dx + \alpha \int_\Omega \left(\sqrt{\frac{A(u^* + t)}{f}} - 1 \right)^2 \, dx$$
$$+ \lambda \int_\Omega |D(u^* + t)|.$$

Concerning $A1 = 1$, we necessarily have:

$$e(t) = \int_\Omega \left(\log(Au^* + t) + \frac{f}{Au^* + t} \right) \, dx + \alpha \int_\Omega \left(\sqrt{\frac{Au^* + t}{f}} - 1 \right)^2 \, dx + \lambda \int_\Omega |Du^*|.$$

Since $t = 0$ is a (local) minimizer of $e(t)$, we have $e'(0) = 0$, which leads to:

$$\int_\Omega \left[\frac{1}{Au^*} - \frac{f}{(Au^*)^2} + \alpha \left(\frac{1}{f} - \frac{1}{\sqrt{f \cdot Au^*}} \right) \right] \, dx = 0.$$

(ii) With $\alpha = 0$ the result in (i) becomes:

$$\int_\Omega \frac{f}{(Au^*)^2} \, dx = \int_\Omega \frac{1}{Au^*} \, dx.$$

Moreover, according to Hölder's inequality and the nonnegativity of Au^* and f, we obtain:

$$\int_\Omega \frac{f}{(Au^*)^2} \, dx \cdot \int_\Omega \frac{1}{f} \, dx \geq \left(\int_\Omega \frac{1}{Au^*} \right)^2 \, dx.$$

Combining both, we have:

$$\int_\Omega \frac{1}{f} \, dx \geq \int_\Omega \frac{1}{Au^*} \, dx.$$

□

Proposition 4.5 indicates that in general the mean of the original image is not automatically preserved under the model (4.1). In order to reduce the influence from the bias and keep the restored image as the same scale as f, we can improve the model (4.1) as:

$$\inf_{\{u \in \bar{S}(\Omega) : m_\Omega(u) = m_\Omega(f)\}} \int_\Omega \left(\log Au + \frac{f}{Au} \right) \, dx + \alpha \int_\Omega \left(\sqrt{\frac{Au}{f}} - 1 \right)^2 \, dx + \lambda \int_\Omega |Du|. \tag{4.4}$$

It is straightforward to show that the feasible set $\{u \in \bar{S}(\Omega) : m_\Omega(u) = m_\Omega(f)\}$ is closed and convex, then the existence and uniqueness of a solution to (4.4) are easily obtained by extending Theorem 4.2.

In (4.4), we implicitly suppose that:

$$m_\Omega(u) \approx m_\Omega(Au), \quad m_\Omega((Au)\eta) \approx m_\Omega(Au).$$

Under some independence conditions, the above assumptions are theoretically rooted in statistics. Moreover, in the practical simulations, we find that these two assumptions provide rather reasonable results.

5. Primal-Dual Algorithm. Since the model (4.4) is convex, there are many methods that can be extended to solve the minimization problem in (4.4). For example, the alternating direction method [8,20], which is convergent and is well-suited to large-scale convex problems, and its variant, the split-Bregman algorithm [23], which is widely used to solve the L^1 regularization problems such as the TV regularization. In this section, we introduce the primal-dual algorithm to solve the minimization problem in (4.4). It extends earlier work in [12,19,31].

We focus on the discrete version of (4.4). For the sake of simplicity, we keep the same notations from the continuous context. Then the discrete model reads as follows:

$$\min_{u\in X} E_A(u) := \langle \log Au, 1\rangle + \left\langle \frac{f}{Au}, 1\right\rangle + \alpha \left\| \sqrt{\frac{Au}{f}} - 1 \right\|_2^2 + \lambda\|\nabla u\|_1, \tag{5.1}$$

where $X = \{v \in \mathbb{R}^n : v_i \geq 0 \text{ for } i = 1,\cdots,n, \text{ and } \sum_{i=1}^n v_i = \sum_{i=1}^n f_i\}$, n is the number of pixels in the images, $f \in X$ is obtained from a two-dimensional pixel-array by concatenation in the usual columnwise fashion, and $A \in \mathbb{R}^{n\times n}$. Moreover, the vector inner product $\langle u, v\rangle = \sum_{i=1}^n u_i v_i$ is used, and $\|\cdot\|_2$ denotes the l^2-vector-norm. The discrete gradient operator $\nabla \in \mathbb{R}^{2n\times n}$ is defined by:

$$\nabla v = \begin{bmatrix} \nabla_x v \\ \nabla_y v \end{bmatrix},$$

for $v \in \mathbb{R}^n$ with $\nabla_x,\ \nabla_y \in \mathbb{R}^{n\times n}$ corresponding to the discrete derivative in the x-direction and y-direction, respectively. In our numerics, ∇_x and ∇_y are obtained by applying finite difference approximations for the derivatives with symmetric boundary conditions in the respective coordinate directions. In addition, $\|\nabla v\|_1$ denotes the discrete total variation of v, which is defined as:

$$\|\nabla v\|_1 = \sum_{i=1}^n \sqrt{(\nabla_x v)_i^2 + (\nabla_y v)_i^2}.$$

Define the function $G : X \to \mathbb{R}$ as:

$$G(u) := \langle \log Au, 1\rangle + \left\langle \frac{f}{Au}, 1\right\rangle + \alpha \left\| \sqrt{\frac{Au}{f}} - 1 \right\|_2^2.$$

Based on the definition of total variation in Section 2, we give the primal-dual formulation of (5.1):

$$\max_{p\in Y} \min_{u\in X} G(u) - \lambda\langle u, \operatorname{div} p\rangle, \tag{5.2}$$

where $Y = \{q \in \mathbb{R}^{2n} : \|q\|_\infty \leq 1\}$, $\|q\|_\infty = \max_{i\in\{1,\cdots,n\}} \left|\sqrt{q_i^2 + q_{i+n}^2}\right|$ denotes the l^∞-vector-norm, p is the dual variable, and the divergence operator $\operatorname{div} = -\nabla^\top$.

This is a generic saddle-point problem, and we can apply the primal-dual method proposed in [12] to solve the above optimization task. The algorithm is summarized as follows.

Algorithm for solving the model (5.1)

1: Fixed σ, τ. Initialize $u^0 = f$, $\bar{u}^0 = f$ and $p^0 = (0, \cdots, 0)^\top \in \mathbb{R}^{2n}$.
2: Calculate p^{k+1} and u^{k+1} from:

$$p^{k+1} = \arg\max_{p \in Y} \; \lambda \langle \bar{u}^k, \operatorname{div} p \rangle - \frac{1}{2\sigma} \|p - p^k\|_2^2, \tag{5.3}$$

$$u^{k+1} = \arg\min_{u \in X} \; G(u) - \lambda \langle u, \operatorname{div} p^{k+1} \rangle + \frac{1}{2\tau} \|u - u^k\|_2^2, \tag{5.4}$$

$$\bar{u}^{k+1} = 2u^{k+1} - u^k. \tag{5.5}$$

3: Stop; or set $k := k + 1$ and go to step 2.

In order to apply the algorithm to (5.1), the main questions are how to solve the optimization problems in (5.3) and (5.4). For (5.3), the solution can be easily given by:

$$p_i^{k+1} = \pi_1 \left(\lambda \sigma (\nabla \bar{u}^k)_i + p_i^k \right), \quad \text{for } i = 1, \cdots, 2n, \tag{5.6}$$

where π_1 is the projector onto the l^2-normed unit ball, i.e.,

$$\pi_1(q_i) = \frac{q_i}{\max(1, |q_i|)} \quad \text{and} \quad \pi_1(q_{n+i}) = \frac{q_{n+i}}{\max(1, |q_i|)}, \quad \text{for } i = 1, \cdots, n,$$

with $|q_i| = \sqrt{q_i^2 + q_{i+n}^2}$.

In addition, since the minimization problem in (5.4) is strictly convex, it can be solved efficiently by the Newton method following with one projection step,

$$u_i^k := \frac{\sum_{j=1}^n f_j}{\sum_{j=1}^n \max(u_j^k, 0)} \max(u_i^k, 0), \quad \text{for } i = 1, \cdots, n, \tag{5.7}$$

to ensure that u^k is nonnegative and preserves the mean of f. This projection is inspired by Prop. 2.1 of [15] or Prop. 12 of [16].

Based on Theorem 1 in [12], we end this section by the convergence properties of our algorithm. The proof refers to [12].

PROPOSITION 5.1. *The iterates* (u^k, p^k) *of our algorithm converge to a saddle point of* (5.2) *provided that* $\sigma\tau\lambda^2 \|\nabla\|^2 < 1$.

According to the result $\|\nabla\|^2 \le 8$ with the unit spacing size between pixels in [10], we only need $\sigma\tau\lambda^2 < \frac{1}{8}$ in order to keep the convergent condition. In our numerical practice, we simply set $\sigma = 3$ and $\tau = 3$, which in most cases ensures the convergence of the algorithm.

6. Numerical Results. In this section we provide numerical results to study the behavior of our method with respect to its image restoration capabilities and CPU-time consumption. Here, we compare our method with the one proposed in [3] (AA method) by solving (1.3) and the one in [32] (RLO method) by solving (1.2), and both of them are able to remove the multiplicative noise and deblurring simultaneously. Since in the AA method and the RLO method the mean of the original image is not preserved, in order to compare fairly, we add the same projection step as in (5.7) before outputting the results. For illustrations, the results for the 256-by-256 gray level images "Phantom", "Cameraman" and "Parrot", are presented, see the original test images in Figure 6.1. The quality of the restoration results is compared quantitatively by means of the peak signal-to-noise ration (PSNR) [7], which is a widely used image quality assessment measure. In addition, all simulations listed here are run in Matlab 7.12 (R2011a) on a PC equipped with 2.40GHz CPU and 4G RAM memory.

(a) (b) (c)

FIG. 6.1. *Original images. (a) "Phantom", (b) "Cameraman", (c) "Parrot".*

Images	Methods	$K = 10$			$K = 6$		
		PSNR(dB)	♯Iter	Time(s)	PSNR(dB)	♯Iter	Time(s)
Phantom	AA	29.44	3000	30.39	27.20	3000	30.73
	RLO	29.37	3000	36.92	27.08	3000	37.77
	Ours	30.44	132	6.09	28.05	174	8.24
Cameraman	AA	24.38	3000	31.09	23.20	3000	33.64
	RLO	24.31	3000	37.99	23.11	3000	37.88
	Ours	25.01	162	8.50	23.85	168	11.82
Parrot	AA	24.53	3000	27.86	23.23	3000	29.14
	RLO	24.28	3000	36.60	22.96	3000	39.61
	Ours	25.47	179	9.19	24.21	219	11.70

TABLE 6.1

The comparisons of PSNR values, the number of iterations and CPU-time in seconds by different methods for denoising case.

6.1. Image denoising. Although our method is proposed as a method for the simultaneous deblurring and denoising of images subject to multiplicative noise, here we show that it also provides very good results for noise removal only. In this example, the test images are corrupted by multiplicative noise with $K = 10$ and $K = 6$, respectively. The results are shown in Figure 6.2-6.4. For the AA method and the RLO method, we use the time-marching algorithm to solve the minimization models as proposed in [3, 32]. We set the step size as 0.1 in order to obtain a stable iterative procedure. The algorithms are stopped when the maximum number of iterations is reached. In addition, after many experiments with different λ-values in the model (1.3) and (1.2), the one with the best PSNR are presented here. In our method, we stop the iterative procedure as soon as the value of the objective function has no big relative decrease, i.e.,

$$\frac{E(u^k) - E(u^{k+1})}{E(u^k)} < \varepsilon.$$

In denoising case, we set $\varepsilon = 5 \times 10^{-4}$.

From Figure 6.2 and 6.3, we can see that all three methods are monotonic decreasing, and our method performs best visually with the least iterations. Note that in the restored results by the AA method and the RLO method, much more noise remains comparing with the ones by our method; see, e.g., white boundary of phantom

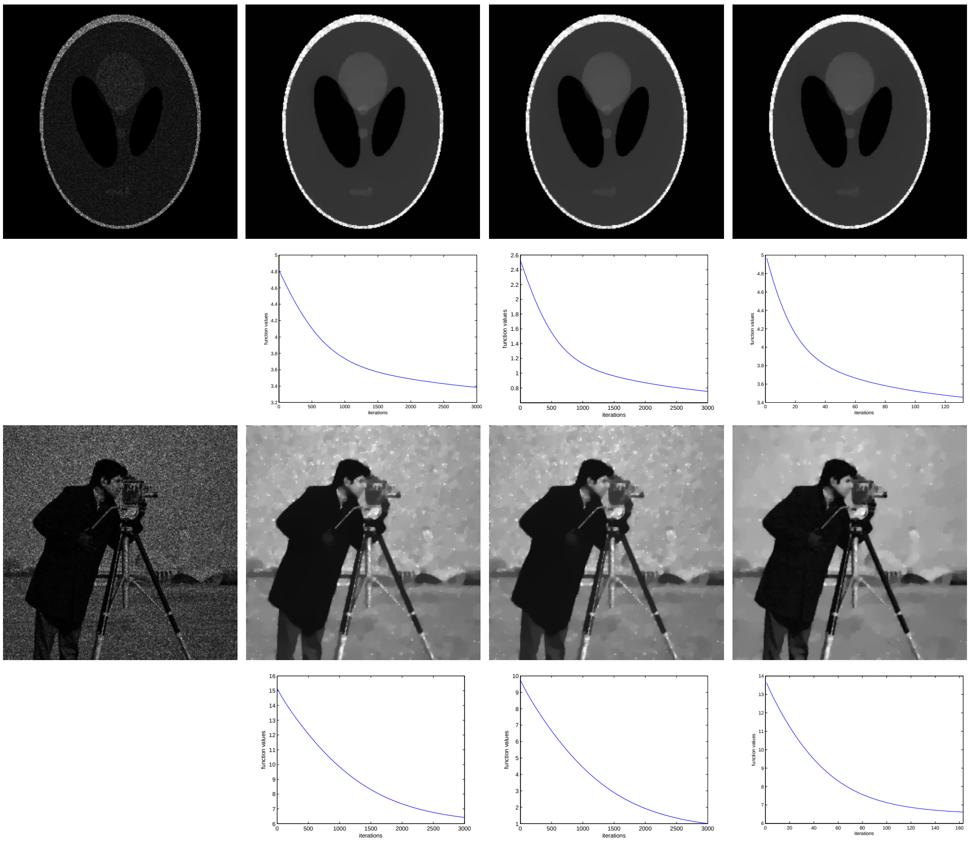

(a) (b) (c) (d)

Fig. 6.2. *Results of different methods when removing the multiplicative noise with $K = 10$. Row 1 and 3: restored images with different methods. Row 2 and 4: the plots of the objective function values versus iterations. (a) Noisy images, (b) AA method (row 1: $\lambda = 0.1$; row 3: $\lambda = 0.14$), (c) RLO method (row 1: $\lambda = 0.12$; row 3: $\lambda = 0.14$), (d) our method (row 1: $\lambda = 0.11$ and $\alpha = 8$; row 3: $\lambda = 0.12$ and $\alpha = 16$).*

and the background in "Cameraman". Moreover, the contrasts of the details by the AA method and the RLO method are noticeably reduced because of oversmoothing during noise removal, however, our method preserves more details. In this respect observe the tripod and the trousers in "Cameraman", especially when recovering the images corrupted by high-level noise. In order to compare the capability of recovering details, in Figure 6.4 we show the results for denoising the image "Parrot" which includes more details. Comparing the textures surrounding the eye and the background of the parrot, we can clearly see that our method suppress noise successfully while preserving significantly more details.

For the comparison of the performance quantitatively and the computational efficiency, in Table 6.1 we list the PSNR values of the restored results, the number of the iterations and the CPU-times. We observe that the PSNR values from our method are more than 0.65 dB higher than others. Due to a large step size, with much less iterations our method reaches to the stopping rule and also spends much less CPU-times. However, in order to obtain a stable iterative procedure, the AA

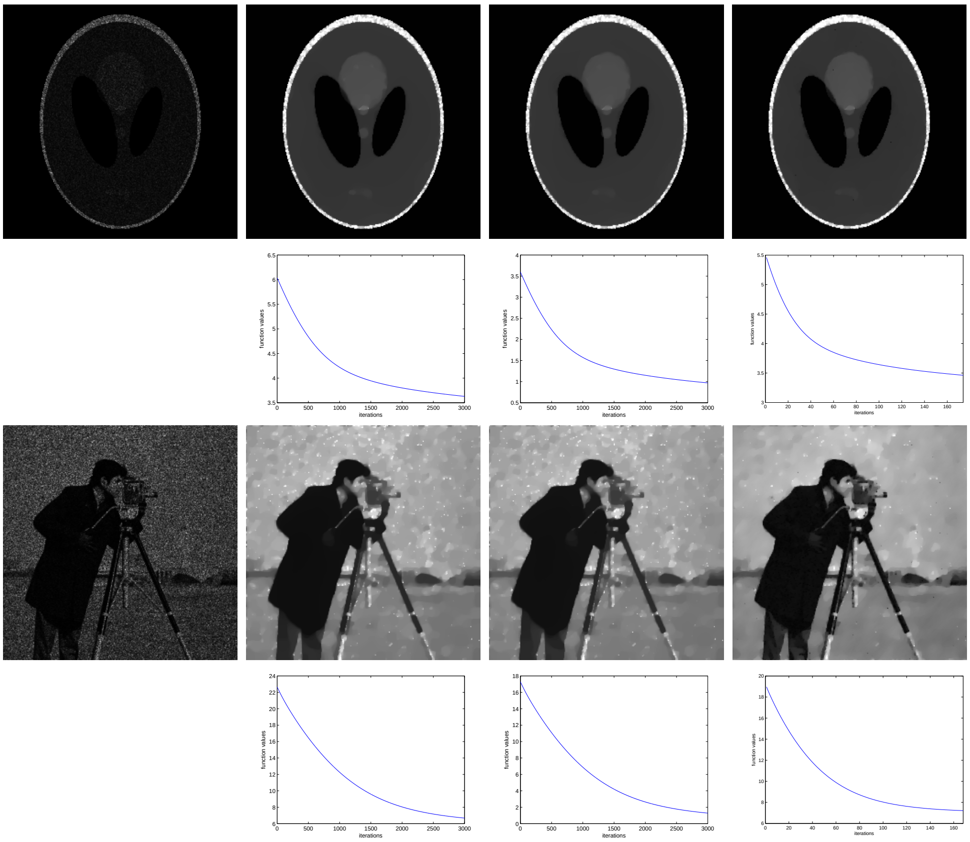

(a) (b) (c) (d)

FIG. 6.3. *Results of different methods when removing the multiplicative noise with $K = 6$. Row 1 and 3: restored images with different methods. Row 2 and 4: the plots of the objective function values versus iterations. (a) Noisy images, (b) AA method (row 1: $\lambda = 0.13$; row 3: $\lambda = 0.2$), (c) RLO method (row 1: $\lambda = 0.13$; row 3: $\lambda = 0.2$), (d) our method (row 1: $\lambda = 0.11$ and $\alpha = 4$; row 3: $\lambda = 0.16$ and $\alpha = 16$).*

method and the RLO method have to use a small step size, and then need more than 10 times more iterations to provide the results with the best PSNR.

6.2. Image deblurring and denoising. In this section, we consider to restore the noisy blurred images. In our experiments, we test two blurring operators, which are motion blur with length 5 and angle 30, and Gaussian blur with a window size 7×7 and a standard deviation of 2. Further, after blurred, the test images are corrupted by multiplicative noise with $K = 10$.

In Figure 6.5-6.7, we show the degraded images and the restored results by all three methods, and Table 6.2 lists the PSNR values, the number of iterations, and the CPU-times. In contrast to the results by the AA method and the RLO method, our method also performs best both visually and quantitatively, and it preserves more details; see, e.g., the tripod in "Cameraman" and the texture near the eye in "Parrot". Due to the blurring, more iterations are needed in all three methods, but our method still provides the best results in much less iterations with the least CPU-times. In a conclusion, our method turns out to be more efficient and outperforms

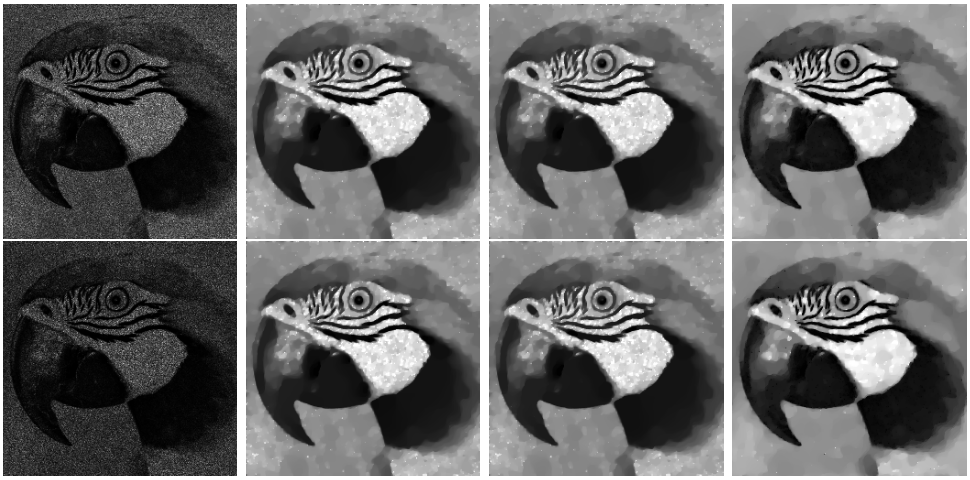

(a) (b) (c) (d)

FIG. 6.4. *Restored images by different methods for restoring the image "Parrot" with different noise level (row 1: with $K = 10$; row 2: with $K = 6$). (a) Noisy images, (b) AA method (row 1: $\lambda = 0.14$; row 2: $\lambda = 0.18$), (c) RLO method (row 1: $\lambda = 0.14$; row 2: $\lambda = 0.18$), (d) our method (row 1: $\lambda = 0.11$ and $\alpha = 16$; row 2: $\lambda = 0.12$ and $\alpha = 8$).*

		Motion Blur			Gaussian Blur		
Images	Methods	PSNR(dB)	♯Iter	Time(s)	PSNR(dB)	♯Iter	Time(s)
Phantom	AA	22.58	8000	223.36	21.12	10^4	289.23
	RLO	22.28	7000	216.14	20.81	10^4	311.00
	Ours	24.68	182	84.78	22.59	331	152.85
Cameraman	AA	22.36	8000	224.71	21.36	10^4	298.34
	RLO	22.28	8000	248.93	21.31	10^4	313.67
	Ours	22.99	200	91.93	21.85	293	119.09
Parrot	AA	22.35	9000	263.82	21.35	10^4	296.58
	RLO	22.15	9000	285.12	21.23	10^4	317.76
	Ours	23.18	216	100.86	22.08	223	103.92

TABLE 6.2

The comparisons of PSNR values, the number of iterations and CPU-time in seconds by different methods for deblurring with denoising.

the other methods which are able to deblurring while removing multiplicative noise simultaneously.

7. Conclusion. In this paper, we focus on variational method to restore the blurred images corrupted by multiplicative Gamma noise. The classical model for this task is non-convex and thus revokes numerical difficulty. In order to overcome this difficulty, based on the analysis of the statistical properties of multiplicative Gamma noise, we propose a new variational model by adding an extra quadratic term. The new model is proved that under certain condition it is strictly convex, even for the deblurring case. Some important properties of the new model, such as the maximal principle and bias correction, are studied in the paper. Further, a primal-dual method is extended to solve our convex model, and the convergent condition is given. The numerical results show that the new method outperforms several recently proposed

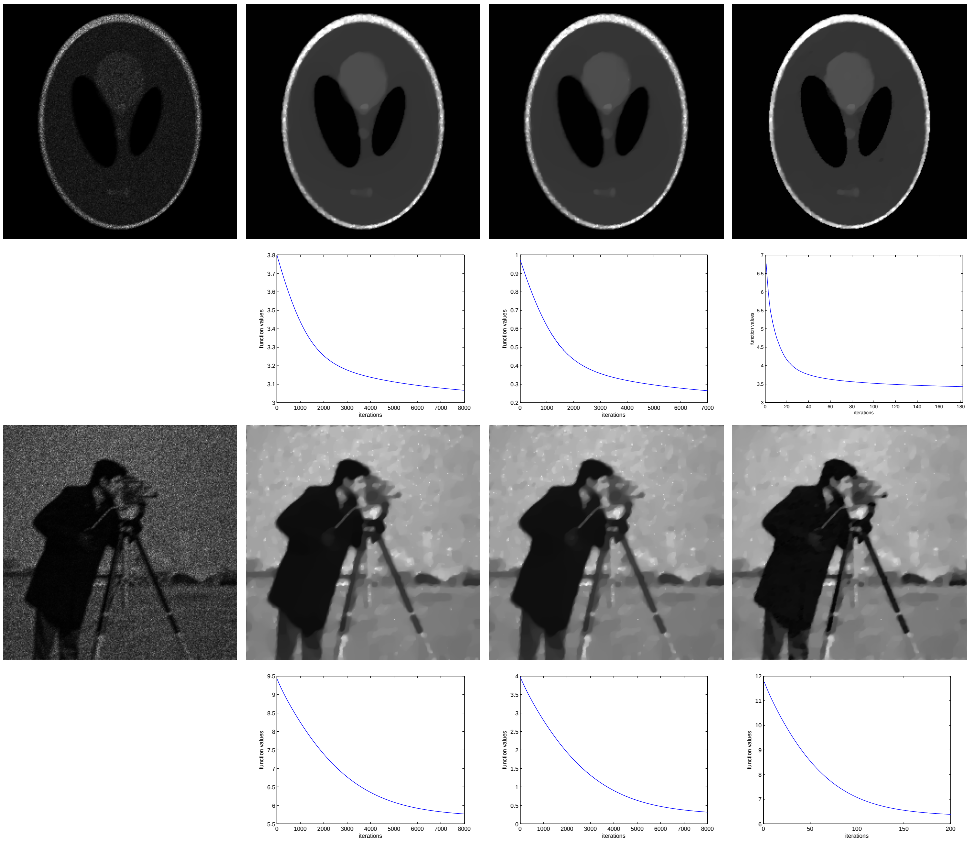

(a) (b) (c) (d)

FIG. 6.5. *Results of different methods when restoring the degraded images corrupted by motion blur and then multiplicative noise with $K = 10$. Row 1 and 3: degraded and restored images with different methods. Row 2 and 4: the plots of the objective function values versus iterations. (a) Degraded images, (b) AA method (row 1: $\lambda = 0.05$; row 3: $\lambda = 0.06$), (c) RLO method (row 1: $\lambda = 0.05$; row 3: $\lambda = 0.06$), (d) our method (row 1: $\lambda = 0.09$ and $\alpha = 16$; row 3: $\lambda = 0.09$ and $\alpha = 16$).*

methods with respect to image restoration capabilities and CPU-time consumption.

Acknowledgement. This work is supported by RGC 211710, RGC 211911, the FRGs of Hong Kong Baptist University.

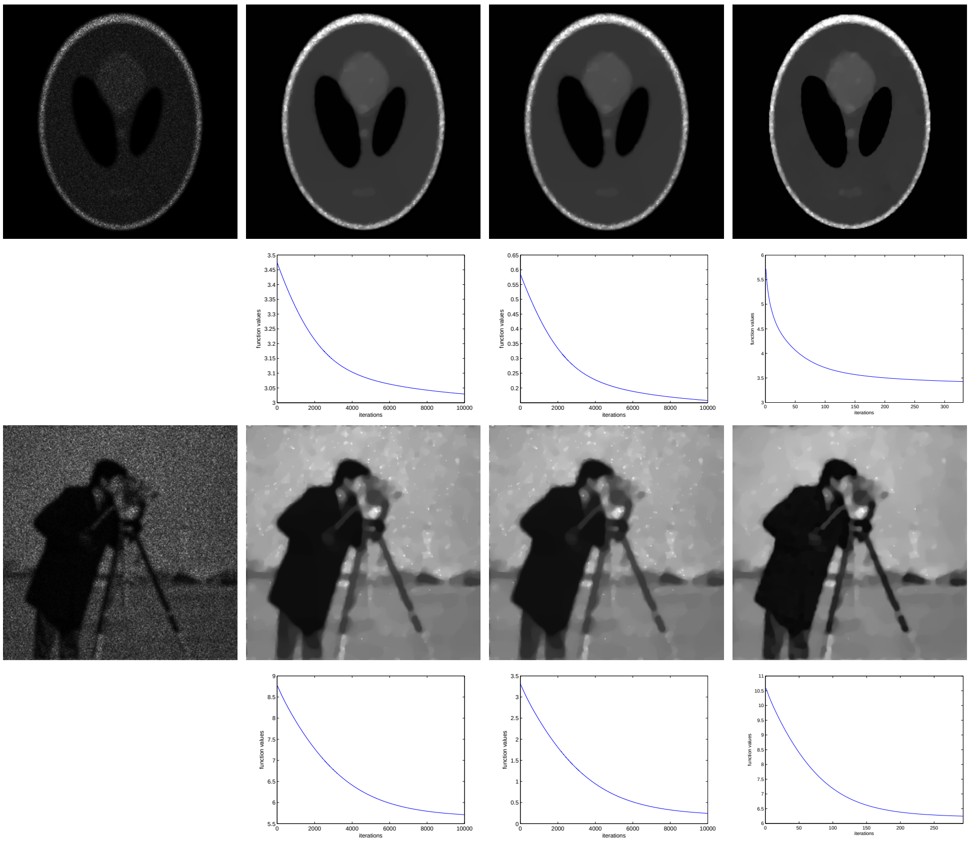

(a) (b) (c) (d)

Fig. 6.6. *Results of different methods when restoring the degraded images corrupted by Gaussian blur and then multiplicative noise with* $K = 10$. *Row 1 and 3: degraded and restored images with different methods. Row 2 and 4: the plots of the objective function values versus iterations. (a) Degraded images, (b) AA method (row 1:* $\lambda = 0.03$*; row 3:* $\lambda = 0.05$*), (c) RLO method (row 1:* $\lambda = 0.03$*; row 3:* $\lambda = 0.05$*), (d) our method (row 1:* $\lambda = 0.07$ *and* $\alpha = 16$*; row 3:* $\lambda = 0.07$ *and* $\alpha = 16$*).*

REFERENCES

[1] L. Ambrosio, N. Fusco, and D. Pallara. *Functions of Bounded Variation and Free Discontinuity Problem*. Oxford university press, 2000.

[2] G. Andrews, R. Askey, and R. Roy. *Special Functions*. Cambridge University Press, 2001.

[3] G. Aubert and J. Aujol. A variational approach to remove multiplicative noise. *SIAM J. Appl. Math.*, 68:925–946, 2008.

[4] G. Aubert and P. Kornprobst. *Mathematical Problems in Image Processing: Partial Differential Equations and the Calculus of Variations*, volume 147. Springer, 2006.

[5] J. Bioucas-Dias and M. Figueiredo. Total variation restoration of speckled images using a split-bregman algorithm. In *Proc. IEEE ICIP*, 2009.

[6] J. Bioucas-Dias and M. Figueiredo. Multiplicative noise removal using variable splitting and constrained optimization. *IEEE Trans. Image Process.*, 19:1720–1730, 2010.

[7] A. Bovik. *Handbook of Image and Video Processing*. Academic Press, 2000.

[8] S. Boyd, N. Parikh, E. Chu, B. Peleato, and J. Eckstein. Distributed optimization and statistical learning via the alternating direction method of multipliers. *Found. and Trends Mach. Learning*, 3:1–122, 2010.

[9] J. Cai, R. Chan, and Z. Shen. A framelet-based image inpainting algorithm. *Appl. Comput.*

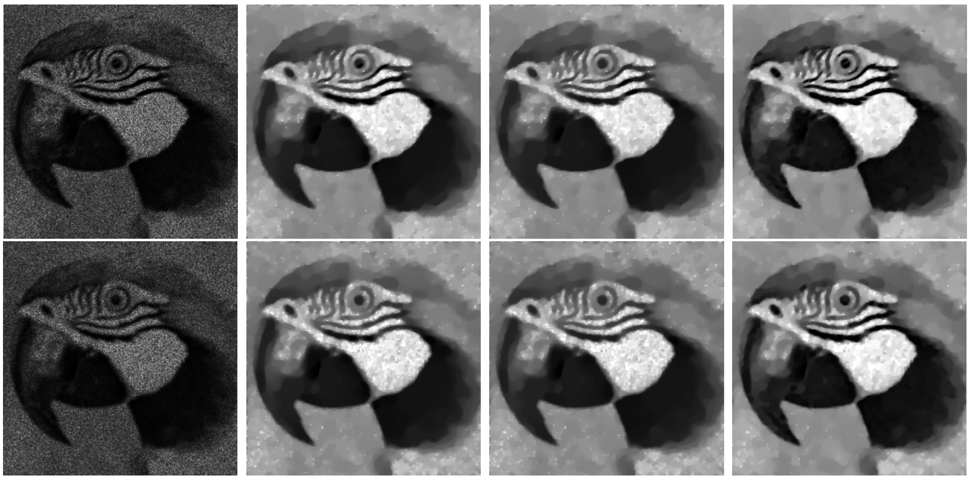

(a) (b) (c) (d)

Fig. 6.7. *Results by different methods for restoring the image "Parrot" blurred by different kernel and then corrupted by multiplicative noise with $K = 10$ (row 1: by motion blur; row 2: by Gaussian blur). (a) Degraded images, (b) AA method (row 1: $\lambda = 0.05$; row 2: $\lambda = 0.04$), (c) RLO method (row 1: $\lambda = 0.05$; row 2: $\lambda = 0.04$), (d) our method (row 1: $\lambda = 0.08$ and $\alpha = 16$; row 2: $\lambda = 0.07$ and $\alpha = 16$).*

Harmon. Anal., 24:131–149, 2008.

[10] A. Chambolle. An algorithm for total variation minimization and application. *J. Math. Imaging Vis.*, 20:89–97, 2004.

[11] A. Chambolle and P. Lions. Image recovery via total variation minimization and related problems. *Numerische Mathematik*, 76, 1997.

[12] A. Chambolle and T. Pock. A first-order primal-dual algorithm for convex problems with applications to imaging. *J. Math. Imaging Vis.*, 40(1):120–145, 2011.

[13] T. Chan and J. Shen. *Image Processing And Analysis: Variational, Pde, Wavelet, And Stochastic Methods*. SIAM, 2005.

[14] T. Chartrand and T. Asaki. A variational approach to reconstructing images corrupted by poisson noise. *J. Math. Imaging Vis.*, 27:257–263, 2007.

[15] C. Chaux, J. Pesquet, and N. Pustelnik. Nested iterative algorithms for convex constrained image recovery problems. *SIAM J. Imaging Sci.*, 2:730–762, 2009.

[16] P. Combettes and J. Pesquet. A douglas-rachford splitting approach to nonsmooth convex variational signal recovery,. *IEEE J. Selected Topics in Signal Processing*, 1:564–574, 2007.

[17] Y. Dong, M. Hintermüller, and M. Neri. An efficient primal-dual method for l1-tv image restoration. *SIAM J. Imaging Sciences*, 2:1168–1189, 2009.

[18] S. Durand, J. Fadili, and M. Nikolova. Multiplicative noise removal using l1 fidelity on frame coefficients. *J. Math. Imaging Vis.*, 36:201–226, 2010.

[19] E. Esser, X. Zhang, and T. Chan. A general framework for a class of first order primal-dual algorithms for convex optimization in imaging science. *SIAM J. Imaging Sci.*, 2010.

[20] M. Figueiredo and J. Bioucas-Dias. Restoration of poissonian images using alternating direction optimization. *IEEE Trans. Image Process.*, 19:3133–3145, 2010.

[21] G. Gilboa and S. Osher. Nonlocal operators with applications to image processing. *Multiscale Model. Simul.*, 7:1005–1028, 2009.

[22] E. Giusti. *Minimal Surfaces and Functions of Bounded Variation*. Birkhäuser, Boston, 1984.

[23] T. Goldstein and S. Osher. The split bregman algorithm for l1 regularized problems. *SIAM J. Imaging Sciences*, 2:323–343, 2009.

[24] G. Grimmett and D. Welsh. *Probability: an introduction*. Oxford Science Publications, 1986.

[25] J. Hadamard. *Sur les problèmes aux dérivées partielles et leur signification physique*. Princeton University Bulletin, 1902.

[26] Y. Huang, M. Ng, and Y. Wen. A new total variation method for multiplicative noise removal. *SIAM J. Imaging Sciences*, 2:20–40, 2009.

[27] P. Kornprobst, R. Deriche, and G. Aubert. Image sequence analysis via partial differential equations. *J. Math. Imaging Vis.*, 11(1):5–26, 1999.

[28] T. Le, R. Chartrand, and T. Asaki. A variational approach to reconstructing images corrupted by Poisson noise. *J. Math. Imaging Vis.*, 2007.

[29] F. Li, M. Ng, and C. Shen. Multiplicative noise removal with spatially varying regularization parameters. *SIAM J. Imaging Sci.*, 3:1–20, 2010.

[30] A. Mood. *Introduction to the Theory of Statistics*. McGraw Hill, 1974.

[31] T. Pock, D. Cremers, H. Bischof, and A. Chambolle. An algorithm for minimizing the mumford-shah functional. In *Proc. 12th IEEE Int'l Conf. Computer Vision*, pages 1133–1140, 2009.

[32] L. Rudin, P. Lions, and S. Osher. *Geometric Level Set Methods in Imaging, Vision, and Graphics*, chapter Multiplicative denoising and deblurring: theory and algorithms, pages 103–119. Springer, 2003.

[33] L. Rudin, S. Osher, and E. Fatemi. Nonlinear total variation based noise removal algorithms. *Physica D*, 60:259–268, 1992.

[34] J. Shi and S. Osher. A nonlinear inverse scale method for a convex multiplicative noise model. *SIAM J. Imaging Sciences*, 1:294–321, 2008.

[35] G. Steidl and T. Teuber. Removing multiplicative noise by douglas-rachford splitting methods. *J. Math. Imaging Vis.*, 36:168–184, 2010.

[36] T. Teuber and A. Lang. Nonlocal filters for removing multiplicative noise. In *SSVM*, volume 6667, pages 50–61. Springer, 2011.

[37] Y. Xiao, T. Zeng, J. Yu, and M. Ng. Restoration of images corrupted by mixed gaussian-impulse noise via $l_1 - l_0$ minimization. *Pattern Recognition*, 44(8):1708–1728, 2011.

[38] T. Zeng and M. Ng. On the total variation dictionary model. *IEEE Trans. Image Process.*, 19(3):821–825, 2010.